

# Recent Progress on Conventional and Non-Conventional Electrospinning Processes

W. S. Khan, R. Asmatulu\*, M. Ceylan, and A. Jabbarnia

*Department of Mechanical Engineering, Wichita State University, Wichita, KS 67260-0133, USA*

(Received February 2, 2013; Revised February 16, 2013; Accepted February 18, 2013)

**Abstract:** Electrospinning is a process of producing micro- and nanoscale fibers using electrostatically charged polymeric solutions under various conditions. Most synthetic and naturally occurring polymers can be electrospun using appropriate solvents and/or their blends. Because of the fascinating properties of electrospun fibers, electrospinning has recently attracted enormous attention worldwide. Initially, this method did not receive much industrial attention due to lower production rates, costs, and lack of interest in size, shape, and flexibility of electrospun nanofibers. However, with the advancement of needleless electrospinning, multiple needles in series, near-field electrospinning techniques, and nanotechnology in particular, this is no longer an issue. This paper outlines the recent progress on the production of various sizes and shapes of fibers using conventional and non-conventional electrospinning processes (e.g., rotating drum and disc, translating spinnerets, rotating strings of electrodes in polymeric solutions, and forcespinning) and presents a complete view of electrospun fiber productions techniques and the resultant products' applications in different fields to date.

**Keywords:** Conventional and non-conventional electrospinning processes, Recent progress, Applications

## Introduction

### General Background

Electrospinning is a process of producing sub-micron and nanosize fibers with high surface area that have superior physical properties (e.g., mechanical, electrical, and thermal) in comparison to their bulk-size fibers. Electrospinning is related to the principle of spinning polymer solutions in a high DC electric field. Nearly all synthetic and naturally occurring polymers can be electrospun when appropriate conditions are provided. In electrospinning, a high-voltage or high-electric field is used to overcome the surface tension of the polymeric solutions. When the intensity of the electric field is increased beyond a certain limit, called threshold intensity, the hemispherical surface of the polymer solution at the tip of the capillary tube begins to elongate in a structure known as a Taylor cone [1]. Electrospun fibers are created from the plastic stretching of a jet of polymeric solution, while the solvent evaporates and the polymer solidifies at micro- and nanoscales on a grounded surface.

The term "electrospinning" was derived from "electrostatic spinning" because an electrostatic field is used to fabricate fibers; the use of this term has increased since 1994 [2,3]. Formhals first patented the electrospinning process in 1934 [2]. In 1969, Taylor studied the shape of the polymeric droplet at the tip of the capillary and demonstrated that a jet is ejected from the vertex of the cone [1]. Following this discovery, most researchers around the world focused on the fabrication and characterization of the electrospun fibers. Electrospinning is a relatively easier and direct process of fabricating a non-woven mat of polymer fibers compared to conventional methods such as melt spinning, wet spinning,

extrusion molding, etc. It offers the distinct advantage of forming fibers in the micro to nano range, and presents a high surface area-to-volume ratio compared to conventional fiber-forming techniques [4].

Electrospinning is not a new technique of manufacturing submicron-size fibers. It has been in use since the 1930s; however, it never gained substantial industrial importance in the last several decades, owing to the low productivity and lack of interest in the resultant products. Today, the special needs of biomedical, filtration, sensor, textile, and military applications have reinvigorated interest in this technique [5,6]. Electrospinning utilizes a high-electric field (or high-electric force) on the surface of a polymeric solution to produce a very slim-charged jet. A polymeric solution is held by its surface tension at the end of the capillary tube. The liquid meniscus emerging from the capillary (capillary stress) has a stress on the order of  $\gamma/r$ , where  $\gamma$  is the surface tension of the polymeric solution, and  $r$  is the radius of the meniscus. The stress induced as a result of the applied field (Maxwell stress) can be given by the Maxwell stress tensor as

$$\sigma_{ij} = \varepsilon V_i V_j + \frac{1}{\mu_0} B_i B_j - \frac{1}{2} \left( \varepsilon V^2 + \frac{1}{\mu_0} B^2 \right) \delta_{ij} \quad (1)$$

where  $\varepsilon$  is the permittivity,  $V$  is the applied voltage (spinning voltage),  $B$  is the magnetic field, and  $\delta_{ij}$  is Kronecker's delta. Neglecting the magnetic part and dividing by  $H^2$ , where  $H$  is the distance between capillary tube and collector screen, equation (1) can be reduced to the following form [7]:

$$\sigma = (\varepsilon V^2)/H^2 \quad (2)$$

Other forces acting on the polymeric solution include inertia, hydrostatic pressure, and viscoelastic forces, which

\*Corresponding author: ramazan.asmatulu@wichita.edu

have little effect compared to the high-electrostatic force and therefore can be mostly neglected. Balancing the Maxwell stress and capillary stress would yield the critical spinning voltage  $V_c$  that must be overcome to initiate electrospinning [7]:

$$V_c = \sqrt{\frac{\gamma H^2}{r \epsilon}} \quad (3)$$

Polymeric solutions are usually electrospun at 7-10 kV DC; however, in order to produce fibers at nanoscale, the applied voltage should be higher than 10 kV. When a charge is applied on the polymeric solution, mutual charge repulsion induces longitudinal stresses because the point charges cannot be maintained in a static equilibrium. This is known as Earnshaw's theorem.

When the intensity of the electrostatic field surpasses the threshold limit ( $V_c$ ), the hemispherical shape of the droplet emerging from the capillary tube transforms into a conical shape, called a Taylor cone [1,8]. First the jet extends linearly for some distance (2-3 cm), called the jet length [9,10], and then instability takes place beyond the relaxation of the jet, where the jet bends and follows a conical spiral looping path (Figure 1) [9]. The reason for this bending instability is the interactions of the charges in the electrified jet. The electrostatic field elongates the jet thousands of times and becomes very slim, usually in the nano range. Finally, the solvent evaporates, and the fine fibers are collected on a screen placed at some distance from the capillary tube.

Electrospun nanofibers have diameters ranging from 500 nm to as low as 3 nm. The main advantage of electrospinning is its ability to produce nanofibers in a shorter period of time. A large variety of sizes and shapes of fibers can be fabricated from numerous polymers. The morphology and surface features of electrospun fibers can be controlled by changing the system and process parameters. The electrospinning process involves many branches of science and technology: mechanical, electrical, chemical, polymer science, fluid mechanics, rheology, and material science [9].

Polymer nanofibers are being used in many applications: filtration [11,12], protective clothing [13], biomedical including wound dressing [14,15], artificial blood vessels [16,17],

sutures, and drug-delivery systems [9]. Other applications include solar cells, fuel cells, batteries, supercapacitors, light sails, photonic devices, and mirrors [9,18]. Nanofibers also offer tremendous advantages in applications such as pesticide controls for plants, structural elements in artificial organs, scaffolds for growing cells, improved food protections [9,19], supports for enzymes or catalysts that can promote chemical reactions, and reinforcements for composites [9,20,21]. The surface of electrospun nanofibers can be modified by coating them with a variety of substances. Nanofibers can be used as templates for making small tubes. Ceramic or carbon nanofibers made from polymer precursors extend nanofiber applications involving high temperature (thermophoto-voltaic generators and high-modulus composites) [22,23]. Ceramic electrospun fibers are made by either a sol-gel mixture or a mixture of inorganic and organometallic compounds with a guide polymer. In addition, polymeric electrospun nanofibers can be coated with a solution of inorganic metallics and organometallics. In all of these cases, electrospun nanofibers are fired to remove the organic substances in an ambient condition and then converted into ceramic electrospun nanofibers [9].

Many substances can be incorporated into the electrospinning process to fabricate nanocomposite nanofibers. Some small insoluble particles can be dispersed into a solution prior to being electrospun. These particles can be encapsulated in dry nanofibers. Polymer nanofibers and nonwoven mats of nanofibers provide the matrix that supports additives/inclusions. Many useful substances can be incorporated into electrospun nanofibers. Different polymers dissolved in the same solvent can be electrospun simultaneously, forming nanofibers with the polymers in separate phases [9].

### Pioneering Studies

Electrospinning is not a new technology. The phenomenon that a spherical drop of water on a dry surface is drawn into a cone when a piece of electrically charged rubber amber is held a suitable distance above it was pointed out 369 years ago by William Gilbert [1]. This was the beginning of the electrospinning process. Rayleigh [9,25,26] studied the hydrodynamic stability mechanism of a liquid jet in the presence and absence of an applied electrostatic field. In 1882, he examined the instability mechanism in an electrified liquid jet and showed that the electrostatic force overcomes surface tension, which acts in the opposite direction, and liquid is thrown out in the form of fine jets [9]. In 1960, Taylor [24,27,28] studied the disintegration of water drops and demonstrated that a conical interface between two fluids could not exist in an equilibrium state under an electrostatic field. He found that droplets elongate at the onset of bending instability at its end and are transformed into a conical shape with a semi-vertical angle of  $49.3^\circ$ . This was the first suggestion for the development of the Taylor cone, which was then extensively discussed by other researchers around

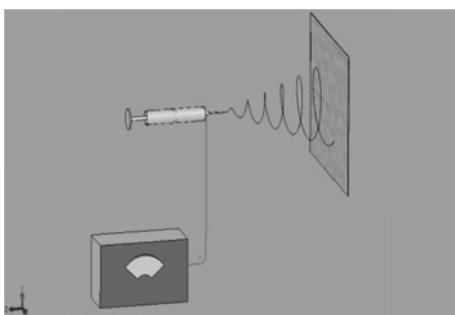


**Figure 1.** Conical spiral looping formation during electrospinning process.

the world [9].

The electrospinning of a polymeric solution has been done since the 1930s [29,30]. Some patents by Formhals [29,31] contain different experimental setups, the collection of electrospun fibers, and their applications during those times. Bumgarten [32] in 1971 and Subbiah *et al.* [33] in 2005 were successful in generating electrospun microfibers using a polyacrylonitrile/dimethylformamide solution. The polymer solution was suspended from a stainless steel capillary tube, and a high voltage was applied. The authors observed that the diameter of the jet reaches a minimum value with an initial increase in the applied voltage and then increases with an increase in the applied field. Larrondo and Manley [33] studied the relationship between melt temperature and fiber diameter of polyethylene and polypropylene, and found that fiber diameter decreased by increasing the melt temperature. In 1987, Hayati [33] demonstrated the effects of an electrostatic field, process conditions, and process parameters on electrospun fibers. He found that the conducting polymeric solution with a high-applied electrostatic field produced an unstable jet, which looped around and whipped in different directions.

Doshi [34] in 1994 and Doshi and Reneker [34,35] in 1995 studied the electrospinning behavior of polyethylene oxide (PEO). Srinivasan [36] and Srinivasan and Reneker [37] electrospun a liquid crystal system poly solution (p-phenyleneterephthalamide) in sulfuric acid and an electrically conducting polymer poly (aniline) in sulfuric acid. The real surge in the electrospinning process began in 1995, when Reneker and co-workers began publishing several papers on the electrospinning process and its potential applications in many industries [9]. Chun [38] in 1995 and Fong *et al.* [39] in 1999 used the electrospinning technique to produce nanofibers from several polymeric solutions, such as poly (amic acid) and poly (acrylonitrile).

In 1996 and 1998, Jaeger and co-workers [40,41] electrospun poly (ethylene oxide) fibers and used scanning probe microscopy to characterize electrospun fibers. In 1997 and 1999, respectively, Fang and Reneker [43] and Fong [42] used a polymeric solution of nylon 6 and polyimide to produce nanofibers via electrospinning. Kim and Reneker [21] in 1999 and Xu *et al.* [20] in 2007 electrospun polybenzimidazole nanofibers and studied the reinforcement effects on electrospun nanofibers in a rubber and epoxy matrix. In 1998, a silicone polyester composite vascular graft was fabricated by an electrospinning technique by Stenoien [44]. Zarkoob [45] in 1998 and Zarkoob *et al.* [46] in 2004 used an electrospinning technique to produce silk nanofibers and compared them with naturally occurring silk fibers. In 2000, Huang and co-workers [47] studied the electrospinning of a synthetic elastin-mimetic peptide.

Reneker *et al.* [18] and Fong *et al.* [39] demonstrated the electrospinning of beaded nanofibers of poly (ethylene oxide). Gibson *et al.* [48] studied the transport properties of

electrospun fiber mats and found that nanofiber layers offer less resistance to moisture vapor diffusional transport. In 2001, Diaz *et al.* [49] fabricated a conducting electrospun mat by blending a conducting material, polyaniline, which was doped with camphorsulfonic acid with poly (ethylene oxide). The conductivity of the electrospun mat was found to be lower than the cast film, due to the porosity effects of the fiber texture. Kim and Lee [50] studied the thermal characterization of electrospun polynaphthalene terephthalate, polyethylene terephthalate, polyester, and polyethylene terephthalate-co-polynaphthalene terephthalate. Bognitzki *et al.* [51, 52] electrospun polylactide from organic solutions in dichloromethane with the addition of an organosoluble, such as tetraethyl benzylammonium chloride or poly(ethylene oxide). A decrease in fiber diameter was observed in this mixture. In 2000, Drew *et al.* [53] electrospun sulfonated polystyrene, and enzymatically synthesized polyaniline and their blends into nanofibers. In 2001, Frank used the electrospinning process to make nanocomposite fibrils with carbon nanotubes [9]. In 1998, Spivak and Dzenis applied nonlinear rheological constitutive equations applicable to polymer fluids to the electrospinning process [54].

Electrospinning of biodegradable polymers and biopolymers has generated considerable interest of many researchers, some of whom have published promising results [55] on collagen and their use as band-aids. Several patents on the biomedical applications of electrospun fibers have been reported recently; notable among them are the ones filed by Woraphan and coworkers [56], wherein they produced a skin mask by directly electrospinning fibers onto the skin surface in order to eventually heal wounds. Another patent [57] claims the production of electrospun fibers containing pH-adjusting compounds for wound treatment or protection from external contaminations.

In 2003, poly (ethylene terephthalate-co-ethylene isophthalate) copolymers, poly (hexyl isocyanate), cellulose, poly (3, 4 ethylenedioxythiophene), and acrylonitrile-butadiene-styrene were electrospun from different polymeric solutions [9]. The incorporation of antimicrobial agents in electrospun fibers, such as silver nanoparticles and Mefoxin, was investigated by Xu *et al.* [58]. In this modern era, the electrospinning technique has drawn the attention of many researchers and scientists around the world. In 2004, more than 300 research papers were published on electrospinning. For more than a decade, these figures have increasingly grown every year. A sudden rise in research on electrospinning is due to the latest knowledge in the industrial applications of nanofibers. Several companies, such as Donaldson, Espin, Star, and Nanomatrix, are applying this technology to produce nanofibers for various applications.

### Theory of Bending Instability

When an external electrostatic field is applied to a polymeric solution, the positive and negative ions move in

opposite directions. Negative ions move toward the positive electrode, and vice versa. The difference in the number of positive and negative ions in a polymeric solution is known as excess charge. Some polymeric solutions are highly insulating; therefore, salt-like potassium chloride is added to dissociate it into equal numbers of positive and negative ions, thereby increasing the ionic conductivity of the polymeric solution by increasing the number of ions per unit volume without increasing the excess charge. The higher conductivity usually shortens the time required for the excess charge, in the form of ions, to move in a particular direction in response to the applied field. When the electrostatic field is applied to the polymeric solution, the surface of the solution is charged, thereby causing the migration of ions through the solution where the jet is formed [59]. The jet emerging from the capillary tube first follows a straight path, or jet length. After some time, segments of a loop develop sequentially bending instabilities. Each cycle of bending instability can be described in three steps [59]:

- A smooth segment of the jet that was straight suddenly develops an array of bends.
- The segment of the jet in each bend is elongated, and the array of bends becomes a series of spiraling loops with increasing diameters.
- As the perimeter of the loops increases, the cross-sectional diameter of the jet grows smaller. The condition of step 1 is established on a small scale, and the next cycle of bending instability begins.

The cycle of instability was observed to repeat many times at a smaller scale. It was found that increasingly more cycles occur, increasingly reducing the jet diameter and creating nanofibers. After the second cycle, the axis of a particular segment may point in any direction. The jet evaporates during its flight from the capillary tube to the collector screen, and electrospun nanofibers are collected [59]. The reason for the bending instability can be understood in the following way: In the coordinate system that moves with a rectilinear electrified jet, the electrical charges can be regarded as a static system of charges interacting mainly by Coulomb's law. Such systems are unstable, according to the Earnshaw's theorem [59], which states that a collection of point charges

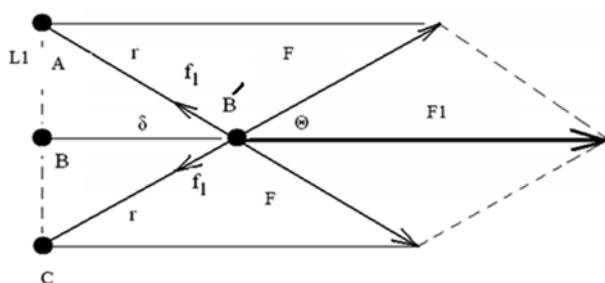


**Figure 2.** Illustration of bending instability using three point charges [59].

cannot be maintained in a static equilibrium solely by their electrostatic interactions. This theorem was first applied to the magnetic field. To explain the instability mechanism, consider three point charges of the same nature, each with a value  $e$  and originally in a straight path line at A, B, and C, as shown in Figure 2 [59].

Two Coulomb forces with a magnitude of  $F=e^2/r^2$  push charge B from the opposite directions, where B moves to B' by a distance  $\delta$ . A force with a magnitude of  $F_1=2F\cos\theta=2(e^2/r^3)\delta$  acts on charge B perpendicular to straight line A, B, and C and causes B to move in the direction of perturbation. The growth of perturbations is governed by the following equation [59]:

$$m \cdot \frac{d\delta^2}{dt^2} = 2e^2 \cdot \delta/L_1^3 \quad (4)$$

where  $m$  is the mass of the jet. The solution of this equation,  $\delta=\delta_0 \exp\{[2e^2/L_1^3 m]^{1/2} t\}$  shows that the small bending perturbations increase exponentially. This increase is sustained because electrostatic energy of the system decreases as  $e^2/r$  when the perturbations characterized by  $\delta$  and  $r$  grow. If charges A, B, and C are attached to a liquid jet, the forces associated with the liquid tend to counteract the instability caused by the Coulomb forces [59].

When the jet becomes unstable at some point from the straight path, both stress relaxation and the number of instabilities occur simultaneously, as shown in Figure 2. The jet undergoes a large reduction in the cross-sectional area, and spiral and whipping motions take place, which is known as the bending/whipping instability of the jet. As a result, the jet can coil and loop itself, as shown in Figure 3 [60]. This type of instability is known as varicose instability, where the centerline of the jet remains straight but the radius of the jet is modulated or changed [60,61]. The last type of instability is the axisymmetric breakdown of a continuous cylindrical

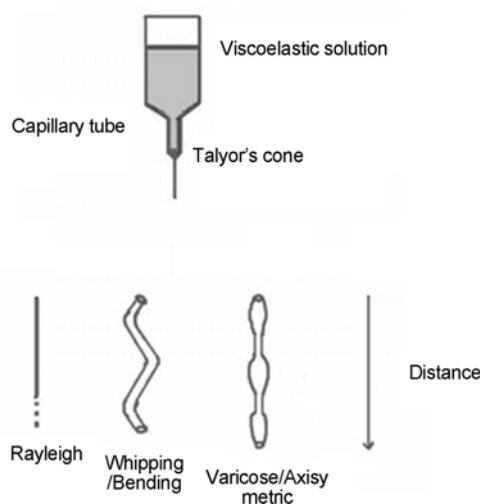


**Figure 3.** Schematic view of various types of instabilities emerging from Taylor cone [60].

column of liquid into spherical droplets, which is known as Rayleigh instability. Rayleigh instability explains the fact that a stream of liquid can break up into a small droplet if its length is greater than its diameter. This type of instability can be suppressed at a high electric field [60,61].

Depending upon the applied field and other process parameters, a variety of jets can emerge from the Taylor cone, as shown in Figure 4 [60]. In a dripping mode (dripping mode), spherical droplets may emerge from the Taylor cone [60,62]. In a spindle mode, the jet is elongated into thin fibers before breaking up into small droplets. In an oscillating mode, the jet is twisted and drops emerge. In a precession mode, a looping jet is initiated from the capillary tube and then breaks up into many droplets. Generally, electrospinning is carried out by a cone-jet mode [62].

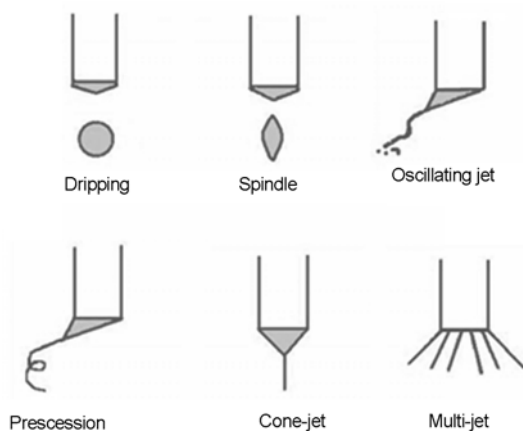


**Figure 4.** Schematic view of various modes of charged jets emerging from Taylor cone [60].

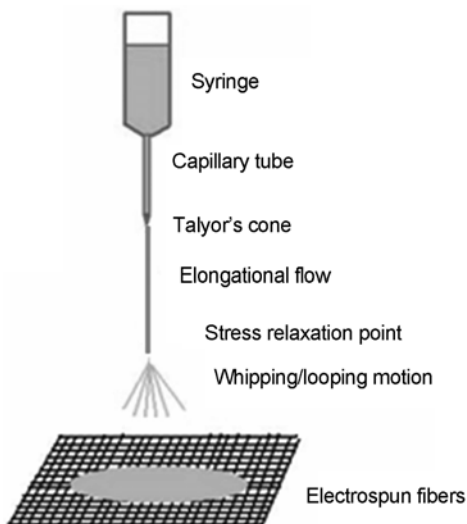


**Figure 5.** Schematic of various regions in electrospinning process [60].

The electrospinning jet is comprised of three regions, as shown in Figure 5: (a) a base, where the jet emerges from the Taylor cone, (b) a region just after the base, where the jet stretches and accelerates, and (c) a collector region, where fibers are collected [60]. The region of interest is where the whipping/looping motion occurs, where the jet splits into numerous sub-jets, reducing the diameter of the jet into submicron size, and then it is finally collected on the collector screen. Shin and coworkers [63] used high-speed photography and confirmed that the unstable region of the jet has the appearance of an “inverted cone,” suggesting that an envelope is created by the multiple jets. They also confirmed that the inverted cone is a single whipping jet [63].

### Electrospinning for Random Oriented Nonwoven Fibers

#### Initial Electrospinning Process

In the electrospinning process, when the electric field reaches a critical value, the repulsive force overcomes the surface tension, and a continuous charged jet of liquid is ejected from the tip of the cone. The repulsive forces are caused by the interaction of the applied electric field with the jet's electrical charge. The ions in the liquid polymeric solution move in response to the electrostatic field and transfer to a force. The drift velocity of the charge carriers in a liquid polymeric solution is the product of the electrostatic field and the mobility of the charge carriers [85].

Generally, charge carriers in a polymeric solution have low mobility, but in the region where the polymeric solution is moving at a high velocity (higher than the drift velocity of charge), they move at the velocity of the surrounding molecules [85]. Rayleigh estimated the maximum charge that a droplet of polymeric solution can hold before the electrostatic field surpasses the forces associated with the surface tension [85]. Roth and Kelly described the evaporating droplet as numerous small droplets carrying away approximately 5 % of the mass and 25 % of the charge [85].

The thinning of a jet caused by bending instability is associated with the change in electrostatic force per surface area of the fiber. The jet begins to stretch and whip around forming a single nanofiber as it travels to the grounded collector screen. Most of the solvent evaporates during the jet's flight to the screen [8]. The electrospinning technique is similar to the commercial process of making microscale fibers except for the fact that electrostatic repulsion is used between surface charges rather than a mechanical or shear force as the drawing force. A syringe pump can control the flow rate of the polymeric solution. The distance between the grounded collector and the tip of the capillary can be altered. Generally, a higher distance (20-30 cm) between the grounded collector and capillary tip is used. Figure 6 shows a schematic view of a conventional electrospinning process.

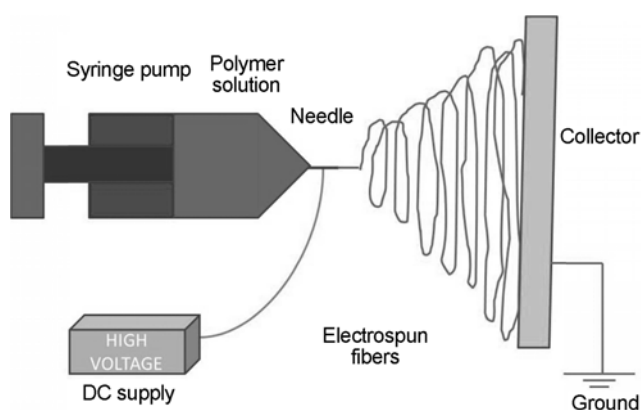


**Figure 6.** Schematic view of conventional electrospinning process.

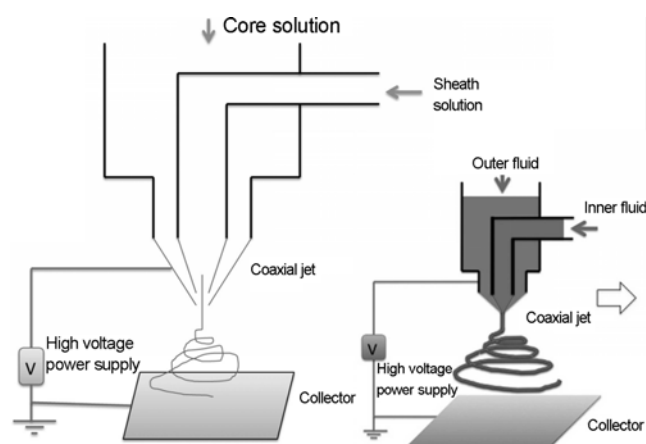


**Figure 7.** Schematic view of coaxial electrospinning.

### Coaxial Electrospinning Processes

Coaxial electrospinning is an extended form of electrospinning. Coaxial electrospinning consists of a central tube nozzle and a nozzle on one side of the central tube nozzle. Two polymeric solutions for the core and sheath materials are separately fed into the central tube nozzle from which they are ejected simultaneously [64]. A compound droplet emerges from the central nozzle, as shown in Figure 7.

When a high electrostatic field is applied, a compound Taylor cone emerges, which consists of core material surrounded by sheath material, and the jet experiences the same bending instability as in traditional electrospinning followed by the evaporation of a jet. Finally, the jet solidifies and is collected on a collector screen in the form of one fiber [64].

### Needleless Electrospinning Process

Electrospinning is a low-production process; therefore, efforts to improve the productivity of electrospinning are being made, such as increasing the number of needles (multiple needle setup) and using the air jacket to improve

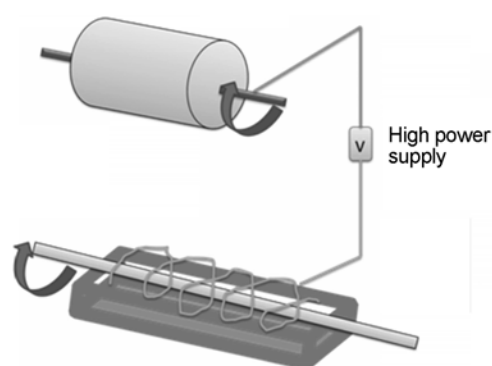


**Figure 8.** Schematic of needleless electrospinning process.

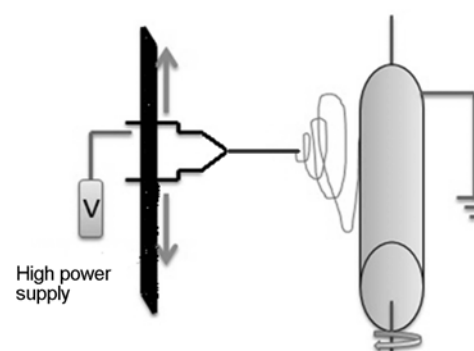


**Figure 9.** Schematic of electrospinning with rotating drum and translating spinneret.

the solution's flow rate [65]. Needle electrospun nanofibers have tremendous industrial applications, but have not been used widely due to the low production rate, i.e., 0.3 g/hr [86]. In needle electrospinning, each nozzle generates only one jet, resulting in a low production rate. In a multiple-needle setup, a large working space is required so that the strong interaction between adjacent jets can be avoided, and a cleaning system must be set up to stop polymeric solution blockage in the nozzles [86].

Recently, needleless electrospinning technology has become a substitute for addressing the issues of low production and a large operating space. Needleless electrospinning (Figure 8) is characterized by direct fibers generated from an open liquid bath. In needleless electrospinning, numerous jets are initiated simultaneously from the liquid bath without any capillary effect, which is commonly observed in needle electrospinning. Since the jet initiation process in needleless electrospinning is self-organized, the spinning process is difficult to control [86]. Spinnerets in needleless electrospinning determine the fibers morphology, fiber quality, and productivity. The experimental setup used in needleless electrospinning is depicted in Figure 9. A copper spiral coil is used as the fiber generator [65]. The bath is filled with polymeric solution, and the coil is rotated in the liquid bath at 40 rpm [65]. The

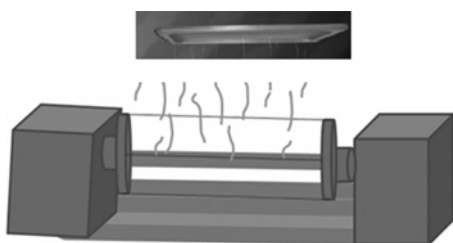


**Figure 10.** Schematic of electrospinning with rotating string of electrodes.

liquid solution is charged by inserting an electrode into the liquid solution, and a rotating drum covered with aluminum foil is used to collect the fibers. Needleless electrospinning produces finer and uniformly oriented fibers with much higher productivity.

### Rotating Drum and Translating Spinneret Electrospinning Process

A continuous and uniform film of fiber can be produced by rotating the collector drum and translating the spinneret. The key parameters in this process are the rotational speed and the translating movement of the spinneret. Conventional electrospinning produces a non-uniform film of fibers. This process has the advantage of a high production rate, better process control, better alignment, and uniformity of fibers. Figure 9 shows a schematic of electrospinning with rotating drum and translating spinneret.

### Rotating Electrodes Electrospinning Process

Another way to improve the production rate of electrospun nanofibers is to rotate the strings of electrodes in the bath of polymeric solution and place a collector screen above it. The electrodes are usually connected to the positive terminal of the power supply, and the collector screen is either grounded or connected to the negative terminal of the power supply. This process eliminates the use of multiple spinnerets and replaces them with strings of electrodes, thus providing a better control process and easy fabrication. This process is cost effective and faster than electrospinning with multiple spinnerets. Figure 10 shows a schematic of electrospinning with a rotating string of electrodes.

## Electrospinning for Oriented Fibers

### Rotating Disk Electrospinning Process

Industrial applications need uniformly oriented fibers without beads and pores. This process produces uniformly aligned fibers without a beaded structure. A uniform film of fibers can be produced by rotating the collector (target), as shown in Figure 11. The jet under the influence of an electrostatic field flows from the tip of the capillary tube to the rotating disk (drum) and experiences bending instability

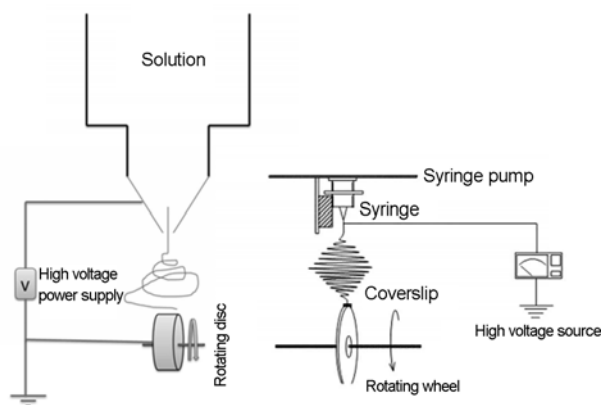


**Figure 11.** Schematic of electrospinning with rotating disk [88].

due to the interactions of surface charges. It is finally gathered onto a rotating disk, which is rotating at a constant velocity. A thick continuous film of nanofibers can be produced in this way.

### Near-Field Electrospinning Process

Conventional electrospinning produces non-woven randomly oriented fibers that have limited industrial applications. However, for industrial applications, the fibers should form uniformly ordered arrays rather than randomly oriented arrays [66]. The main reason for random fiber orientation is the bending instability of the electrified jet in the conventional electrospinning process. Near-field electrospinning (NFES) is an effective process for better fiber alignment and control [66]. In this process, a positive charge is applied to the polymeric solution, and the collector screen is grounded, as in conventional electrospinning. The distance between the capillary tip and the collector screen is reduced. Typically, a distance of 0.5 mm to 3 mm is used. A critical voltage of around 1.4 kV is applied to the polymeric solution in order to introduce a charge to the polymeric solution [66]. With this low voltage, a droplet of polymeric solution forms at the tip of the capillary tube without initiating the electrospinning process [66]. Then an array of sharp tips with diameters of 20  $\mu\text{m}$  is inserted into this droplet and quickly removed, resulting in numerous jets emerging from the droplet [66]. The distance between the two adjacent tips should be more than 50  $\mu\text{m}$  to ensure effective emanating of the jet from the droplet. The repulsive forces between adjacent jets prevent them from merging together. The fibers thus fabricated are orderly oriented. Figure 12 shows a schematic of non-conventional electrospinning.

### Non-Bending Instability Electrospinning Process

High charge density on the electrospun jet is responsible for extensive plastic stretching that results in ultrafine fiber diameters and leads to the unstable and whipping motion of the jet, which is commonly referred to as bending instability

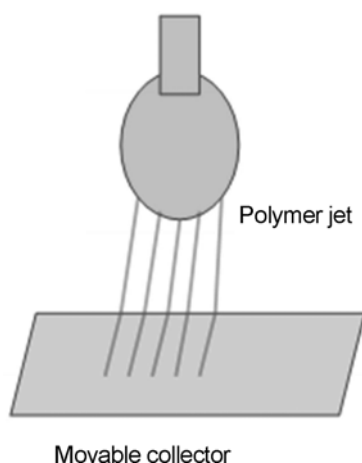


**Figure 12.** Schematic of non-conventional electrospinning process.

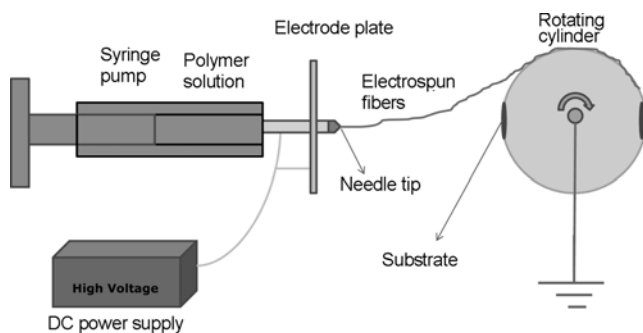


**Figure 13.** Schematic of electrospinning without bending instability.

[83]. Bending instability is observed in the electrospinning process and causes the fibers to form non-woven mats of random orientation [83]. However, for almost all industrial applications, the fibers should form an ordered array rather than random mats. By using a low electrostatic field near the tip of the capillary tube and a low flow rate, and by placing an electrode plate behind the electrospinning emitter, a more uniform electrostatic field that suppresses the bending instability can be created [83]. These well-defined conditions of electrospinning produce continuous fibers. The electrode plate is connected to the same high voltage as the polymer solution in the capillary tube. Figure 13 shows a schematic of electrospinning without bending instability.

### Recent Progress

Since conventional electrospinning is marred by low productivity and uniformity of fibers, a newly developed process called forcespinning addresses these issues. This new process uses centrifugal force to fabricate nanofibers rather than electrostatic force as in conventional electrospinning. The forcespinning process uses either a solution or solid materials that are spun into nanofibers [76]. The parameters that influence the morphology and geometry of fibers are

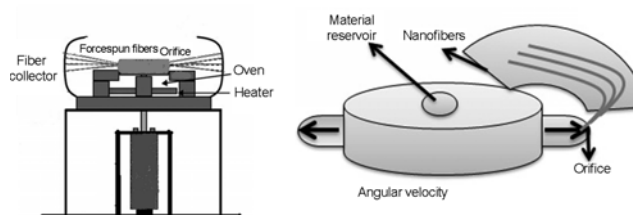


**Figure 14.** Schematic of forcespinning process [90].

rotational speed of the spinneret, collector system, temperature, and geometry of the orifice [76]. In forcespinning, the electric field is replaced by centrifugal force with multiple patterns of interchangeable spinnerets making it a versatile process that overcomes the limitations of the conventional electrospinning process, such as high electrostatic force and the dielectric nature of the solution [76]. Since electrostatic force is not utilized, both conductive and non-conductive solutions can be spun into nanofibers. A number of materials can be melted and spun simultaneously. The polymeric solution or melt is forced through the orifices of the spinneret by centrifugal force. The centrifugal force causes the solution or melts to emerge from the orifices, thus forming continuous jets of polymeric solution and stretching into the formation of a continuous web of ultrafine fibers. This web of continuous fibers is collected on a custom-designed collector system. Figure 14 shows the different arrangements of the forcespinning process.

This versatile technique allows using both polymeric solution and solid materials through orifice to fabricate fibers [89]. The ionic conductivity and electrostatic charges are not critical parameters to fabricate fibers; therefore, the spectrum of materials to be forcespun is considerably broader in comparison to needle spinning. The parameters to be controlled are shape and size of the orifice, angular motion of spinneret and the design of the collection system [89].

### Parameters Affecting Electrospinning Process

Primarily two parameters affect the electrospinning process: system parameters and process parameters. System parameters are associated with the experimental setup before the electrospinning process begins and are based on experience and the literature review. They include parameters such as solvent type, polymer for electrospinning, viscosity, conductivity, dielectric properties, and surface tension of the solution. Process parameters are decided after the experiment is set up. They include parameters such as electrostatic field, mass flow rate, distance between tip of capillary tube to collector screen humidity, temperature, air velocity in the electrospinning chamber, and the polymeric solution concentration. These parameters can be adjusted according to the application. The morphology and surface features of electrospun fibers depend upon these parameters.



### System Parameters

Thus far, all synthetic and naturally occurring polymers have been electrospun. The solvent for electrospinning should be selected on the basis of its properties, such as solubility, conductivity, surface tension, and dielectric constant. The molecular weight of the polymer determines the fiber morphology. A high molecular weight results in a large fiber diameter, and a low molecular weight results in pores and a beaded structure, which are considered defects in fiber formation.

The viscosity of a polymeric solution significantly affects the fiber diameter. Pores, micropores, and beaded structures are less likely to form during electrospinning if the viscosity is high. If the viscosity is too low, the initiating jet from the Taylor cone will be transformed into many droplets, and the jet will experience splashing, thus resulting in beaded structure. If the viscosity is too high, then the viscoelastic forces will be high. As a result, a higher electrostatic force is required to overcome the viscoelastic forces and the jet will be transformed into droplets instead of forming fibers.

Electrospinning depends on rheological properties of the polymeric solution. Increasing the viscosity of the solution reduces the formation of beads and increases the fiber diameter. If the viscosity is above 20 poise, then electrospinning becomes impossible because of the instability of the flow caused by the cohesively of the solution. Droplets are formed when the viscosity is low (<1 poise). A higher electrical conductivity can have significant influence on fiber diameter. In general, small-diameter fibers can be produced with a higher electrical conductivity solution [67]. By reducing the surface tension of the polymeric solution, the fibers produced will be without beaded structures [67]. Different solvents will result in different surface tension. However, a solvent with low surface tension is not always suitable for electrospinning. Generally, a solution with low surface tension helps electrospinning to occur at a low electrostatic field. The viscosity of the polymeric solution and the diameter of the electrospun fiber are related by the following equation [68]:

$$d = 19.49 \eta^{0.43} \quad (5)$$

where  $\eta$  is the viscosity of solution and  $d$  is the diameter of the fiber (nm).

### Process Parameters

During the jet's flight from the tip of the capillary tube to the collector screen, it experiences plastic stretching and evaporation due to natural convection, and as a result, the jet diameter gets smaller before it is collected on the collector screen. A higher electric field results in low fiber diameter, and these two parameters are related by the following equation [69].

$$d \sim V^{-1/2} \quad (6)$$

where  $V$  is the electrical potential. Hendricks [69] calculated the minimum spraying potential of a suspended hemispherical conducting drop in air as

$$V = 300 \sqrt{20 \pi \gamma r} \quad (7)$$

where  $r$  is the radius of the cone, and  $\gamma$  is the surface tension of the polymeric solution. Taylor [69] developed a similar relation for the critical potential as

$$V_c^2 = 4H^2/L^2 \left( \ln \frac{2L}{R} - \frac{3}{2} \right) (0.117 \pi \gamma R) \quad (8)$$

where  $V_c$  is the critical voltage,  $H$  is the separation between the capillary and the ground,  $L$  is the length of the capillary,  $R$  is the radius of the capillary, and  $\gamma$  is the surface tension of the liquid.

The surface features and morphology of electrospun fibers depends upon flow rate of the solution. When the flow rate exceeds the threshold value, the fibers produced are surrounded by beads and pores. The polymer concentration is dependent upon the molecular weight of the polymer. However, concentration can be reduced by increasing the solvent content. The polymer concentration should not be too low or too high, but rather a compromise between maximum and minimum. The fiber diameter increases as the polymer concentration increases. If the polymer concentration is too high, then electrospinning becomes relatively difficult, and a higher electric field would be required to overcome the viscoelastic forces, or pores, micropores, and beads will form.

Polymers with higher molecular have high viscosity in solution form and the resulting electrospun fibers will have large diameters. Molecular weight also greatly influences the rheological properties of the polymeric solution. It has been observed that a low molecular weight solution produces beads and pores due to the low concentration of the solution, and a higher molecular weight solution produces fibers with large diameters due to the high concentration of the solution. The distance between the capillary tube and the collector screen also influences the fiber diameter: a large distance ensures enough time for the jet to undergo plastic stretching resulting in finer fibers.

Generally, electrospinning process takes place at room temperature. At high temperature, the evaporation rate will be high, and thereby fibers having large diameters will be produced. High relative humidity during electrospinning leads to the formation of micropores and nanopores on the surface of the fibers due to the breath figures effect [70]. Quick evaporation of the solvent condenses the moisture present in the air, leaving imprints in the form of micro- and nanopores on the surface of fibers [70]. Some polymers absorb moisture and some do not; therefore, high humidity can decrease or increase the fiber diameter depending upon the polymer used. The presence of moisture in the electrospinning chamber impedes evaporation [70]. High airflow

results in a higher evaporation rate, thus resulting in larger-diameter fibers.

### Applications of Electrospun Fibers

Nanofibers possess some unique properties, all of which make them an ideal material for many industrial applications [2]. These include high aspect ratio, nanosize diameter, good surface morphology, large surface area-to-volume ratio, thermal and chemical stability, low ohm resistance, high porosity, and high directional strength. Biodegradable and biocompatible polymers are finding many biomedical field applications such as tissue engineering and drug delivery. In recent years, electrospun fibers have been extensively investigated as scaffolds in tissue engineering. Biodegradable polymers have benefited in the development of templates or scaffolds for tissue engineering [71].

Synthetic polymeric biomaterials have controlled physico-chemical properties, and they can be synthesized with no immunogenicity. They can also be processed with various techniques and consistently supplied in large quantities. In order to adjust the physical and mechanical properties of tissue-engineered scaffolds at a desired place in the human body, the molecular structure and molecular weight can be easily adjusted during the synthetic process. Some synthetic biodegradable polymers are in the family of poly( $\alpha$ -hydroxy) esters, such as polyglycolide (PGA), polylactide (PLA), its copolymer poly(lactide-co-glycolide) (PLGA), polyphosphazene, polyanhydride, poly(propylene fumarate), polycyanoacrylate, poly( $\epsilon$ -caprolactone) (PCL), polydioxanone (PDO), and biodegradable polyurethanes. Of the two types of synthetic polymers, synthetic biodegradable polymers are preferred for the application of tissue-engineered scaffolds because they minimize the chronic foreign body reaction and lead to the formation of completely natural tissue. They can form a temporary scaffold for mechanical and biochemical support. On the other hand, synthetic biomaterials are generally biologically inert, they have more predictable properties and batch-to-batch uniformity, and they have the unique advantage of having tailored property profiles for specific applications, devoid of many of the disadvantages of natural polymers. Compared to degradable polymers, hydrolytically degradable polymers are generally preferred as implants due to their minimal site-to-site and patient-to-patient variations.

Electrospun nanofibers can be used for wound and burn treatment of human skin [77]. By applying an electrostatic field, ultrafine electrospun fibers of biodegradable polymers can be directly sprayed onto the injury location to form a fibrous mat dressing, which would allow wounds to heal by formation of normal skin growth and prevent the formation of scar tissue [77]. Furthermore, electrospun nanofibers have small pore sizes (500 nm to 1 nm), which can protect wounds from bacterial penetration [77]. Electrospun fibers fabricated from biocompatible polymers are being used to

make tissue scaffolds that can be used for solving critical medical problems of tissue loss or bone repair. Bioabsorbable and biodegradable electrospun nanofibers can be used for targeted drug delivery. Bioabsorbable nanofiber membranes of poly (lactic acid) targeted for the prevention of surgery-induced adhesions can be used for loading an antibiotic drug Mefoxin [77]. Electrospun nanofibers with multiple layers have high porosity and a pore size at nanoscale that can provide good resistance to protecting against harmful chemical agents in aerosol form [77].

Electrospun fibers are used in the textile industry because they have water repellent, durable, soft, fire retardant and anti-microbial properties. Conventional fibers used in the textile industry have diameters in the range of 1 to 100  $\mu\text{m}$  [72]. The fibers produced by electrospinning have diameters in the nano range. Carbon nanotube-reinforced fibers produced by electrospinning provide high strength. Further enhancement in strength and conductivity of electrospun fibers can be achieved by heat treatment. After heat treatment, these fibers can be used as bullet-proof vest and electromagnetic wave-tolerant fabrics [72]. Electrospinning a polymeric solution incorporated with carbon nanotubes using several capillary tubes in series can produce nano-yarns having diameters in the nano range. These highly twisted nano-yarns have high strength, toughness, and energy-damping properties and therefore can be used to produce electronic textiles for supporting multi-functionalities such as energy storage capacity, radio and microwave absorption, capability for actuation, wiring for electronic devices, textile heating, electrostatic discharge protection, etc. [72].

Electrospun nanofibers can be used as superhydrophobic non-woven membranes due to the surface roughness introduced during spinning. Surfaces with special wettability play an important role in our daily lives and in industrial applications as well. Surface roughness and surface energy are the dominant factors for determining the wettability of a surface. A material with the lowest surface energy (6.7 mJ/m<sup>2</sup> for a surface with closed-hexagonal-packed-CF<sub>3</sub> group) provides a water contact angle of 120° [73], whereas a hydrophilic material can produce a surface with a water contact angle of around 150° after surface treatment [73]. The F<sub>3</sub> group has the lowest surface energy when functionalized onto a flat surface, and the water contact angle increases and reaches a value of around 120° [74]. Zheng *et al.* [73] reported a lotus-leaf-like microsphere/nanofiber composite film of polystyrene with superhydrophobic features (water contact angle=160.4°) using the electrohydrodynamics method [73]. Electrospun block copolymer poly (styrene-*b*-dimethylsiloxane) fibers with diameters in the range of 150-40 nm were reported to have superhydrophobicity behavior with a water contact angle of 163° [73]. The superhydrophobicity can be attributed to the surface roughness of the electrospun fibers and the surface enrichment due to siloxane [73]. Kong *et al.* [74] determined that electrospun poly ( $\epsilon$ -caprolactone) with chemical vapor

deposition of polymerized perfluoroalkyl ethyle methacrylate and electrospun poly (styrene-dimethylsiloxane) display superhydrophobicity [74]. Kang *et al.* [74] reported that when polystyrene was electrospun in tetrahydrofuran and chloroform, the water contact angles were 138.1 ° and 138.8 °, respectively, and the water contact angle was remarkably increased to 154.2 °, when polystyrene was electrospun with N, N-dimethylformamide solvent. Ma and co-workers [75] reported the superhydrophobicity (water contact angle= 163 °) of electrospun nonwoven mats composed of submicron fibers of poly (styrene-b-dimethylsiloxane) block copolymer blended with homopolymer polystyrene.

Recently, polymer nanofibers reinforced with carbon nanotubes (CNTs) have received considerable attention because nanofibers have better mechanical properties than microfibers; therefore, superior structural properties of nanocomposites can be anticipated [77]. Zhang *et al.* [78] reported electrospun poly (ethylene oxide) nanofibers with multiwall carbon nanotubes, and continuous nanofibers yarn with CNTs by electrospinning [78]. They found that the modulus increased with the incorporation of CNTs [78]. The miniaturization of electronic devices has increased those problems associated with heat dissipation and demands the improved thermal interface of materials in chip packaging [79]. Heat management in electric motors, generators, heat exchangers, bio and nanosensors, and other electronic and communication devices are also challenging issues [80,81]. Traditionally, metallic materials have been widely used as heat-dissipation materials. Thermally conductive polymer-based electrospun nanocomposites can be a possible alternative to metallic materials due to their light weight, corrosion resistance, low manufacturing cost, and easy fabrication. Therefore, in order to address thermal-management issues in many industries, electrospun polymers incorporated with multiwall carbon nanotubes (MWCNTs) and  $\text{Ni}_{0.6}\text{Zn}_{0.4}\text{Fe}_2\text{O}_4$  (NiZn ferrites) are being investigated by many researchers as a possible alternative to traditional materials.

Nanofiltration (NF) membranes fabricated by electrospun nanofibers have a wide range of applications in filtration. The pore size of a membrane is typically around 1 nm. NF membranes are often used in the softening of ground water and the purification of surface water for producing drinking water [82]. The pore size of NF membranes enables a wide range of industrial applications, particularly as wastewater treatment for textile industries to enable water reuse [82]. NF membranes are capable of size-based separation with sub-nanometer resolution, which could attract significant markets in the chemical, pharmaceutical, and food industries [82]. Recently, a U.S. patent has outlined a method for fabricating a dust filter bag that contains a nanofiber nonwoven layer [77]. Electrospun nanofibers in pulse-clean cartridges for dust collection and in the cabin-air filtration of mining vehicles have also been introduced [77]. Electrospun nanofibers can be electrostatically charged to increase the electrostatic

attraction of particles in order to increase filtration efficiency. Moreover, electrospun nanofiber membranes fabricated from some specific polymers or incorporated with some selected fillers can be used as molecular filters, i.e., for filtration of chemicals and biological agents [77].

Encapsulation is an acceptable process because it enhances the viability of bacteria, allows the handling of cells, and ensures controlled dosage. The common encapsulation techniques are spray-drying and emulsifying-crosslinking. These techniques involve the use of high temperatures and/or organic agents, resulting in the destruction of some sensitive encapsulated nutrients and toxicity problems associated with residual organic agents [84-87]. Therefore, new technology is needed to address the issue of high temperature and toxicity. Electrospinning is a simple and versatile technique to produce fibers and/or capsules in submicron size. Electrospinning does not involve high temperature, although many polymers require an organic solvent for making the polymeric solution before electrospinning. However, some biopolymers can be dissolved in a watery solvent by changing the process parameters and by adding proper additives. This recent advancement has outstanding potential in the food science area for developing novel functional ingredients [84].

## Conclusion

Electrospinning is a novel and straightforward process for producing ultrafine fibers in a short period of time. By controlling the process and system parameters, fibers without beads, pores, and microparticles can be produced using the electrospinning process. The deficiency of low productivity can be eliminated by placing a number of needles in series or needleless electrospinning processes. Conventional electrospinning produces non-woven randomly oriented fibers; however, for industrial applications, orderly oriented uniform fibers are required. Near-field electrospinning is an effective technique for producing fibers having better alignment and control. NFES eliminates the bending instability during plastic stretching of the electrified jet, thereby producing an orderly and uniform film of fibers. In recent years, huge advancements have been made in nanofiber production, such as the rotating drum and translating spinnerets, electrospinning with a rotating string of electrodes, and forcespinning. Electrospinning with a rotating drum and translating spinneret provides better alignment, a faster production rate, and uniformity of nanofibers. Electrospinning with rotating strings of electrodes can enhance the rate of production and better alignment. Forcespinning eliminates the use of high electrostatic force, thus allowing conducting and non-conducting polymeric solutions to be electrospun. Electrospun fibers have several applications in the biomedical, textile, filtration, self-cleaning, and many other industries and these applications will grow dramatically in the near future.

## References

- G. Taylor, *Proceedings of Royal Society of London*, London, **313**, 1515 (1969).
- R. K. Bharath, Ph.D. Dissertation, Miami University, Oxford, Ohio, 2006.
- Z. M. Huang, Y. Z. Zhang, M. Kotaki, and S. Ramakrishna, *Compos. Sci. Technol.*, **63**, 15 (2003).
- H. Fong, I. Chun, and D. H. Reneker, *Polymer*, **40**, 16 (1999).
- J. H. He, Y. Q. Wan, and J. Y. Yu, *Int. J. Nonlinear Sci. Numer. Simul.*, **5**, 3 (2004).
- J. H. Wendorff, S. Agarwal, and A. Greiner, "Electrospinning: Materials, Processing, and Applications", Willy-VCH, Singapore, 2012.
- L. Y. Yeo and J. R. Friend, *J. Experimental Nanoscience*, **1**, 2 (2006).
- E. V. Kalayei, K. P. Patra, A. Bauer, C. S. Ugbohue, K. Y. Kim, and B. S. Warner, *J. Adv. Mater.*, **36**, 4 (2004).
- W. Kataphinan, Ph.D. Dissertation, The University of Akron, Ohio, 2004.
- D. H. Reneker, A. L. Yarin, H. Fong, and S. Koombhongse, *J. Appl. Phys.*, **87**, 9 (2000).
- Y. K. Kang, C. H. Park, J. Kim, and T. J. Kang, *Fiber. Polym.*, **8**, 564 (2008).
- A. D. Vaisniene, J. Katunskis, and G. Buika, *Fibers Text. East. Eur.*, **17**, 6 (2009).
- M. Gorji, A. A. A. Jeddi, and A. A. Gharehaghaji, *J. Appl. Polym. Sci.*, **125**, 5 (2012).
- J. P. Chen, G. Y. Chang, and J. K. Chen, *Colloid. Surface. A: Physicochem. Eng. Aspect.*, **317**, 450 (2008).
- R. A. Thakur, C. A. Florek, J. Kohn, and B. B. Michniak, *Int. J. Pharm.*, **364**, 1 (2008).
- C. Y. Xu, R. Inai, M. Kotaki, and S. Ramakrishna, *Biomaterials*, **25**, 5 (2004).
- L. J. Levy, *U.S. Patent*, 4549545 (1985).
- D. H. Reneker, A. L. Yarin, E. Zussman, and H. Xu, *Adv. Appl. Mech.*, **41**, 42 (2007).
- W. J. Li, C. T. Laurencin, E. J. Caterson, R. S. Tuan, and F. K. Ko, *J. Biomed. Mater. Res.*, **60**, 4 (2002).
- L. R. Xu, L. Li, C. M. Lukehart, and H. Kuai, *J. Nanosci. Nanotechnol.*, **7**, 7 (2007).
- J. S. Kim and D. H. Reneker, *Polym. Compos.*, **20**, 1 (1999).
- P. J. Goldstein, Master's Thesis, University of Florida, Florida, 2004.
- H. Fong and D. H. Reneker, "Electrospinning and Formation of Nanofibers", in *Structure Formation in Polymer Fibers*, (D. R. Salem Ed.), pp.4585-4592, Princeton, Hanser Gardner Publication Inc., 2000.
- C. H. Park, C. H. Kim, L. D. Tijing, D. H. Lee, M. H. Yu, H. R. Pant, Y. Kim, and C. S. Kim, *Fiber. Polym.*, **13**, 339 (2012).
- L. Rayleigh, *Philosophical Magazine Series 5*, **14**, 87 (1882).
- L. Rayleigh, *Proceedings of Royal Society of London*, UK, **29** (1897).
- G. Taylor, *Proceedings of Royal Society of London*, A **28**, UK, 280, 1382 (1964).
- G. Taylor, *Proceedings of Royal Society of London*, A **291** (1966).
- A. Formhals, *US Patent*, 1975504 (1934).
- P. J. Berry, *US Patent*, 5024789 (1991).
- A. Formhals, *US Patent*, 2349950 (1944).
- P. Baumgarten, *J. Colloid Interface Sci.*, **36**, 1 (1971).
- T. Subbiah, S. G. Bhat, W. R. Tock, S. Parameswaran, and S. S. Ramkumar, *J. Appl. Polym. Sci.*, **96**, 2 (2005).
- J. Doshi, Ph.D. Dissertation, University of Akron, Akron, Ohio, 1994.
- J. Doshi and D. H. Reneker, *J. Electrostat.*, **35**, 2 (1995).
- G. Srinivasan, Ph.D. Dissertation, University of Akron, Akron, Ohio, 1994.
- G. Srinivasan and D. H. Reneker, *Polym. Int.*, **36**, 2 (1995).
- I. Chun, Ph.D. Dissertation, University of Akron, Akron, Ohio, 1997.
- H. Fong, I. Chun, and D. H. Reneker, *Polymer*, **40**, 16 (1999).
- R. Jaeger, M. M. Bergshoef, M. C. Ibatlle, H. Schönherr, and J. G. Vansco, "Macromolecular Symposia, Rolduc Polymer Meeting 10", p.127, Netherland, 1998.
- R. Jaeger, H. Schönherr, and G. J. Vansco, *Macromolecules*, **29**, 23 (1996).
- H. Fong, *J. Macromol. Sci. B-Phys.*, **36**, 2 (1997).
- M. D. Stenoien, W. J. Drasler, R. J. Scott, and M. L. Jenson, *U.S. Patent* 5840240 (1998).
- S. Zarkoob, Ph.D. Disertation, University of Akron, Ohio, 1998.
- S. Zarkoob, R. K. Eby, D. H. Reneker, S. D. Hudson, D. Ertley, and W. W. Adams, *Polymer*, **45**, 3973 (2004).
- L. Huang, R. A. McMillan, R. P. Apkarian, B. Pourdeyhimi, V. P. Conticello, and E. L. Chaikof, *Macromolecules*, **33**, 8 (2000).
- P. W. Gibson, H. L. S. Gibson, and D. Rivin, *ALCHE Journal*, **45**, 1 (1999).
- M. Diaz, N. J. Pinto, J. Gao, and A. G. Mac Diarmid, "National Conference of Undergraduate Research", University of Kentucky, Lexington, 2001.
- J. S. Kim and D. S. Lee, *Polymer*, **32**, 7 (2000).
- M. Bognitzki, T. Frese, J. H. Wendorff, and A. Grenier, *219th ACS National Meeting*, San Francisco, CA, PMSE-173, American Chemical Society, Wasington, D.C. 2000.
- M. Bognitzki, T. Frese, J. H. Wendorff, and A. Greiner, *Polym. Mater.: Sci. Eng.*, **82**, 45 (2000).
- C. Drew, X. Wang, K. Senecal, H. Schreuder-Gibson, J. He, S. Tripathy, and L. Samuelson, *Proceedings of the SPE 58th Annual Technical Conference*, 2 (2000).
- A. F. Spivak and Y. A. Dzenis, *Appl. Phys. Lett.*, **73**, 21 (1998).

54. B. Wessling, *Synthetic Metals*, **93**, 2 (1998).
55. K. Woraphan, D. Sally, D. H. Reneker, and S. Daniel, *US Patent*, WO012661, 2001.
56. D. Smith, D. Reneker, A. McManus, H. Schreuder-Gibson, C. Mello, M. Sennett, and P. Gibson, *US Patent*, WO0127365, 2001.
57. H. Liu, Ph.D. Dissertation, University of Georgia, Athens, 2008.
58. X. Xu, Q. Yang, Y. Wang, H. Hu, X. Chen, and X. Jing, *Eur. Polym. J.*, **42**, 2081 (2006).
59. C.-M. Hsu, Master's Thesis, Worcester Polytechnic Institute, Worcester, MA, 2003.
60. M. H. Hohman, M. Shin, G. Rutledge, and M. P. Brenner, *Physics of Fluids*, **13**, 2221 (2001).
61. M. E. T. Molaes, A. G. Balogh, T. W. Cornelius, R. Neumann, and C. Trautmann, *Appl. Phys. Lett.*, **85**, 5337 (2004).
62. Y. N. Shin, M. M. Hohman, M. P. Brenner, and G. C. Rutledge, *Appl. Phys. Lett.*, **78**, 8 (2001).
63. D. Han and A. J. Steckl, *Langmuir*, **25**, 16 (2009).
64. X. Wang, H. Niu, X. Wang, and T. Lin, *J. Nanomater.*, **2012**, 785920 (2012).
65. W. S. Khan, R. Asmatulu, Y. H. Lin, Y. Y. Chen, and J. Ho, *J. Nanotechnol.*, **2012**, 138438 (2012).
66. A. K. Haghi and M. Akbari, *Physica Status Solidi*, **204**, 6 (2007).
67. V. E. Kalayci and P. K. Patra, *J. Adv. Mater.*, **36**, 4 (2004).
68. J. H. He, Y. Q. Wan, and J. Y. Yu, *Int. J. Nonlinear Sci. Numer. Simul.*, **5**, 3 (2004).
69. I. Sas, R. E. Gorga, J. A. Joines, and K. A. Thoney, *J. Polym. Sci.*, **50**, 12 (2012).
70. M. S. Sumitha, K. T. Shalumon, V. N. Sreeja, R. Jayakumar, S. V. Nair, and D. Menon, *J. Macromol. Sci.-A: Pure and Applied Chemistry*, **49**, 2 (2012).
71. A. P. S. Sawhney, B. Condon, K. V. Singh, S. S. Pang, G. Li, and D. Hui, *Text. Res. J.*, **78**, 8 (2008).
72. J. Zheng, A. He, J. Li, J. Xu, and C. C. Han, *Polymer*, **47**, 20 (2006).
73. M. Kong, R. Jung, H. S. Kim, and H. J. Jin, *Colloids Surf. A: Physicochem. Eng. Asp.*, **313-314**, 411 (2008).
74. M. Ma, R. M. Hill, J. L. Lowery, S. V. Fridrikh, and G. C. Rutledge, *Langmuir*, **21**, 12 (2005).
75. K. Sarkar, C. Gomez, S. Zambrano, M. Ramirez, E. de Hoyos, H. Vasquez, and K. Lozano, *Material Today*, **13**, 11 (2010).
76. S., Ramakrishna, "An Introduction to Electrospinning and Nanofibers", World Scientific, Singapore, 2005.
77. N. Nuraje, W. S. Khan, M. Ceylan, Y. Lie, and R. Asmatulu, *Mater. Chem. A*, **1**, 1929 (2013).
78. Q. Zhang, Z. Chang, M. Zhu, X. Mo, and D. Chen, *Nanotechnology*, **18**, 115611 (2007).
79. P. E. Slade and L. T. Jenkins, "Thermal Characterization Techniques," Marcel Dekker, New York, 1970.
80. J. M. Biercuka, C. M. Liaguno, M. Radosavljevic, K. J. Hyunc, T. A. Johnson, and E. J. Fischer, *Appl. Phys. Lett.*, **80**, 15 (2002).
81. D. Hansen and H. C. Chong, *J. Polym. Sci.-A: General Papers*, **3**, 2 (1965).
82. W. S. Khan, R. Asmatulu, and M. B. Yildirim, *J. Aerospace Eng.*, **25**, 3 (2012).
83. F. A. Sheikh, N. A. M. Barakat, M. A. Kanjwal, S. J. Park, H. Kim, and H. Y. Kim, *Fiber. Polym.*, **11**, 384 (2010).
84. A. López-Rubio, E. Sanchez, S. Wilkanowicz, Y. Sanz, and J. M. Lagaron, *Food Hydrocolloids*, **28**, 1 (2012).
85. D. H. Reneker and I. Chun, *J. Nanotechnol.*, **7**, 3 (1996).
86. H. Niu and T. Lin, *Journal of Nanomaterials*, Vol. 2012 (2012), Article ID 725950, p. 13.
87. P. Gupta, R. Asmatulu, G. Wilkes, and R. O. Claus, *J. Appl. Polym. Sci.*, **100**, 4935 (2006).
88. A. Seema, W. H. Joachim, and G. Andreas, *Polymer*, **49**, 26 (2008).
89. V. Beny, V. Horacio, and L. Karen, *Polym. Eng. Sci.*, **52**, 10 (2012).
90. F. Cengiz-Callioglu, O. Jirsak, and M. Dayik, *Fiber. Polym.*, **13**, 1266 (2012).